

Electrical characterization of photocatalytic TiO₂ films

P.R.F. Barnes^{a,b}, P.F. Vohralik^{a,b} and I.C. Plumb^{a,b}

^a CSIRO Industrial Physics, PO Box 218 Lindfield, NSW 2070, Australia.

^b CSIRO Energy Transformed Flagship.

Rutile films were grown on titanium metal sheet by thermal oxidation. The photocatalytic efficiency of the films for splitting water to oxygen and hydrogen was about ten times higher when the titanium substrate had been etched in acid prior to oxidation. Impedance measurements suggest this could be due to higher electron mobilities in the films grown on etched substrates.

1. Introduction

Metal oxide semiconductors offer the prospect of electrochemically stable materials for use as photocatalysts in applications such as solar water splitting. Recently there has been renewed interest in n-type titania as a photoelectrode material due to the possibility of reducing its band-gap to absorb more sunlight [1, 2]. However, large variations in the energy conversion efficiencies of TiO₂ can be attributed to substrate preparation alone, regardless of band gap. The reason for this is unclear.

Changing the stoichiometry of titania allows the material to range from electrically insulating to conducting since oxygen vacancies donate electrons to the conduction band, increasing the charge carrier concentration. The efficiency of converting absorbed photons to electrochemical work will depend on both the number density and mobility of charge carriers available in the oxide [3]. The through-film current-voltage and capacitance-voltage characteristics of the oxide layer should allow these factors to be determined. This work considers the variation of photocatalytic efficiency of TiO₂ (rutile) electrodes with different substrate preparations in view of electrical impedance measurements at room temperature.

2. Experimental

Titania films were prepared by the thermal oxidation of strips of 99.7 % titanium sheet. Prior to oxidation, the surfaces were cleaned in both acetone and deionised water using an ultrasonic bath. In some cases, the sheet was then etched using Kroll's solution (40 % HCl, 20 % HF and 40 % water) for 5 seconds, followed by another ultrasonic cleaning process. The titanium strips were oxidized at 750 °C in oxygen at 0.2 atm pressure for either 10 or 20 minutes in a sealed tube oven. X-ray diffraction measurements indicated the films had a rutile structure. Preparation and characterisation details of the films are shown in Table 1.

The photo-electrochemical performance of the oxide films for splitting water to form hydrogen and oxygen was measured using electrodes prepared under identical conditions to those used for electrical measurement. The procedure for measuring the photocurrent and efficiency is described in detail elsewhere [4, 3].

Electrical contacts were formed by evaporating 2.95 mm diameter aluminium or gold pads onto the surface of the oxide film. Wires were connected to the pads using silver paint to form Al/TiO₂/Ti Ohmic circuits or Au/TiO₂/Ti Schottky diode circuits. Electrical measurements were made using a Radiometer Analytical, VoltaLab PGZ 301 potentiostat.

3. Results and Discussion

The maximum measured photo-electrochemical conversion efficiency, η_{max} , of incident radiant energy (equivalent to AM1.5 sunlight [4]) to stored chemical energy, for films grown on etched and un-etched substrates is shown in Table 1. The results indicate that preparation

of the substrate surface by etching in acid prior to oxidation was the most significant parameter in determining electrode performance – increasing η_{max} by a factor of ten. This cannot be entirely attributed to differing surface roughness of the samples. Atomic force microscope measurements of the specific surface area of the oxide films indicated an increase of only 1.02 to 1.06 for the etched substrate film which is insufficient to explain the observed change in efficiency. However a significant difference can be seen in the electrical properties of the films prepared identically to those used for the photo-electrochemistry. Table 1 shows the through-film conductivity (measured using the aluminium pads) is around 50 times higher for the films grown on etched substrates compared to un-etched.

Figure 1a shows examples of I - V curves obtained using the gold contacts for etched and un-etched samples. The vertical offset between the curves (on the log scale) can be attributed to differing leakage currents, possibly through pinholes with ohmic behaviour. The most significant difference in I - V behaviour between the etched and un-etched samples is in the forward bias region. Here there is a marked increase in slope of $d(\log[I])/dV_{bias}$ above about 0.6 V for etched but not the un-etched films.

The correction for series resistance (R_s) in the film: $V_{bias} = V_{applied} - IR_s$ was small. Variation in diode current density, j , with V_{bias} is empirically expressed as a function of the effective zero bias barrier height of the Schottky junction, Φ , and the diode ideality factor, n :

$$j = A_R^* T^2 \exp(-\Phi/k_B T) \exp(eV_{bias}/nk_B T) [1 - \exp(-eV_{bias}/k_B T)] \quad (1)$$

where T is the temperature, k_B is Boltzmann's constant, e is the electronic charge, and A_R^* is the effective Richardson constant [5]. Fig. 1b shows the linear dependence, predicted by (1), between $\ln[j/(1-\exp(-eV_{bias}/k_B T))]$ and V_{bias} corresponding to curves in Fig. 1a. The slope and intercept should equal $e/nk_B T$ and $A_R^* T^2 \exp(-\Phi/k_B T)$ yielding n and Φ respectively (see Table 1). A change in slope is apparent in Fig. 1b between the forward and reverse bias regions of the curves. In reverse bias the diodes tended towards ideal behaviour; however in forward bias

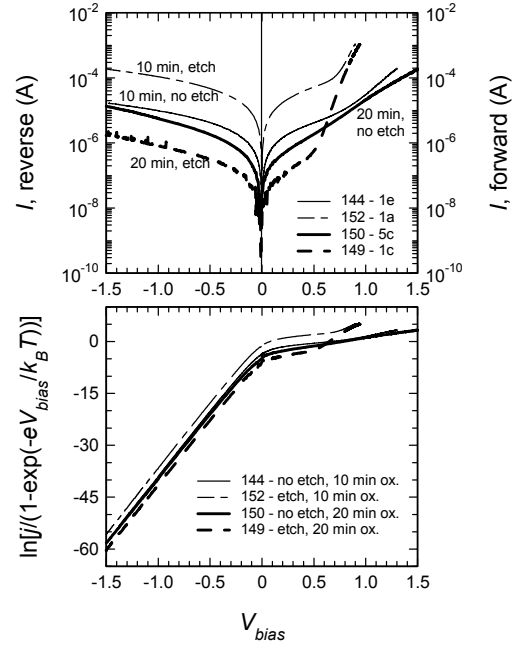


Fig. 1a. Forward and reverse bias current as a function of diode bias for TiO_2 surfaces. b. $\ln[j/(1-\exp(-eV_{bias}/k_B T))]$ plotted against applied bias for the curves shown in a.

Table 1. Summary of preparation and characterisation measurements on TiO_2 films. $\dagger \eta_{max}$ and j_p , the photocurrent density measured when the photoelectrode was set at 0 V versus a standard saturated calomel electrode (SCE), are scaled to values for a solar AM 1.5 spectrum [4]. Φ assumes $A_R^* = 1.2 \times 10^6 \text{ A m}^{-2} \text{ K}^{-2}$. \ddagger The mean high forward bias ideality factor, n , is given in parenthesis where it is significantly different from the low bias value.

Samp. no.	Subs. etched	Ox. time (min)	Film thick. (nm)	η_{max} (%)	V_{bias} at η_{max} (V)	j_p at 0V vs SCE \dagger (mA cm $^{-2}$)	Specific conductance (S m $^{-2}$)	Cond'ty (S m $^{-1}$)	Φ (V) Rev. bias	n Rev. bias	Φ (V) For'd bias	n For'd bias
144	no	10	800	0.04	0.7	0.07	$(4.3 \pm 4.1) \times 10^3$	0.0020	0.65	1.05	0.66	16.1
147	yes	10	700	0.37	0.62	0.67	$(1.1 \pm 0.5) \times 10^5$	0.065	1.04	1.48	0.76	4.4 (1.9)
152	yes	10	420	0.37	0.62	0.67	$(2.1 \pm 1.5) \times 10^5$	0.048	0.62	1.04	0.64	12.0 (2.9)
150	no	20	1100	0.03	0.9	0.08	$(1.1 \pm 0.4) \times 10^3$	0.0010	0.71	1.08	0.79	6.3
149	yes	20	1500	0.27	0.61	0.57	$(3.5 \pm 0.4) \times 10^5$	0.52	0.79	1.09	0.85	4.6 (2.2)
151	yes	20	840	0.27	0.61	0.57	$(4.9 \pm 2.8) \times 10^5$	0.36	0.66	1.04	0.69	10.6 (2.5)

(below about 0.6 V for all samples) the value of n rose to significantly greater than unity, this observation is best explained by significantly inhomogeneous barrier height [5, 6]. The inhomogeneities are likely to arise from both the polycrystalline nature of the oxide and any scratches penetrating the gold films. Measuring n at forward biases greater than about 0.6 V for the etched samples showed a reduction in n compared to the lower bias values in contrast to the un-etched samples. In forward bias these junctions are clearly not well described by simple thermionic emission theory.

The width of the depletion layer at a given bias can be determined using C_{sc} , the space charge capacitance of the film: $w(V_{bias}) = \epsilon_0 \epsilon_r A / C_{sc}(V_{bias})$ where ϵ_0 is the permittivity of free space and ϵ_r is the relative permittivity of the TiO_2 . The carrier concentration profile, $N(w)$ of the film can also be calculated: $N(w) = 2[dV_{bias}/d(1/C_{sc}^2)]/e\epsilon_0\epsilon_r A^2$ [7]. The curves in Fig. 2 indicate that the space charge capacitance measurements probe only a very narrow regions several hundred nanometres below the gold contact. Again there is a clear difference in behaviour observed between the films oxidised on etched and un-etched titanium substrates. In the latter cases there is a very rapid change in carrier concentration over a very short depth range; this presumably results from an abrupt interface between an oxidised region with low defect density and a highly sub-stoichiometric region at the metallic interface. In contrast to this, the films oxidised on etched titanium substrates suggest a much more gradual transition, from a region of low defect density (low N) near the surface of the electrode to a progressively more sub-stoichiometric (higher N) approaching the metallic phase. In both cases the N transition occurs deeper in the layer when the film was oxidised for longer; we conclude from this that, unsurprisingly, increasing the oxidation time increases the stoichiometry of the film close to the specimen surface, allowing the depletion layer to penetrate further into the sample for a given bias.

These results do not directly indicate the charge carrier density close to the sample surface; however we may use the values in Fig. 2 and Table 1 to infer upper limits for the carrier densities in the surface region. A lower limit for the electron mobility in the surface region is then given by $\mu_{min} = \sigma/(eN_{max})$. Using this crude approach we find the lower bound for the effective mobility of electrons within the surface region of the ‘etched’ films appears to be about ten times higher than the ‘un-etched’. This observation at once could account for the observed difference in efficiency between the film types assuming that under operation at maximum efficiency the surface region of the electrode is fully depleted of electrons.

References

- [1] R. Asahi, T. Morikawa, T. Ohwaki, K. Aoki, and Y. Taga, *Science* **293**, 269 (2001).
- [2] P. R. F. Barnes, Lakshman K. Randeniya, A. B. Murphy, P. B. Gwan, I. C. Plumb, J. A. Glasscock, I. E. Grey, and Christina Li, *Dev. Chem. Eng. Mineral Process.* **14**, 51 (2006).
- [3] A. K. Ghosh and H. P. Maruska, *J. Electrochem. Soc.* **124**, 1516 (1977).
- [4] A. B. Murphy, P. R. F. Barnes, M. D. Horne, J. A. Glasscock, I. E. Grey, I. C. Plumb, L. K. Randeniya, *Int. J. Hydrogen Energy* (in press, 2006).
- [5] W. Mönch, *Electronic properties of semiconductor interfaces* (Springer, Germany, 2004).
- [6] R. T. Tung, *Mater. Sci. Eng. R.* **35** 1 (2001).
- [7] D. K. Schroder, *Semiconductor material and device characterization* (Wiley, New York, 1990).

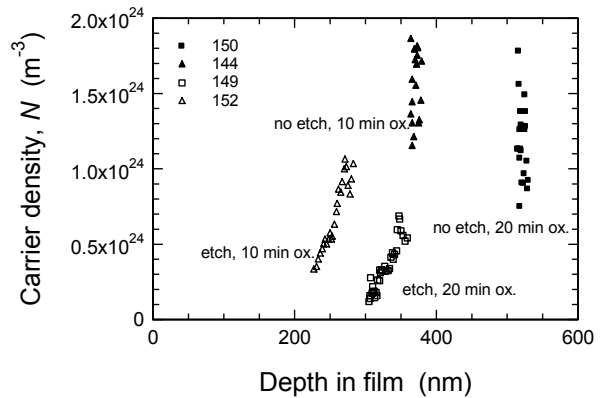


Fig. 2. Charge carrier concentration as a function of depth in TiO_2 films.